PCCP

ROYAL SOCIETY OF CHEMISTRY

PAPER

View Article Online
View Journal | View Issue

Cite this: *Phys. Chem. Chem. Phys.*, 2023, **25**, 10440

Detection of DNA translocations in a nanopore series circuit using a current clamp†

Fei Zheng, Yi Tao, Wei Xu and Jingjie Sha*

Received 28th September 2022,
Accepted 8th March 2023

DOI: 10.1039/d2cp04530c

rsc.li/pccp

The advancement of nanopore sensing technology over the past 20 years has been impressive, particularly in the field of nucleic acid sequencing, which has already been used in commercial diagnostic tests. A traditional configuration of nanopore sensing records the current through a single nanopore using a voltage clamp, which hits a bottleneck in expanding its functions, while integrating several nanopores to build a nanopore circuit may be an effective solution. Here, we report a new strategy combining a nanopore series circuit and a current clamp to record the current signal and the voltage signal of DNA translocation through a nanopore simultaneously, which could increase the fidelity of event analysis. We observed a capacitor-like charging and discharging behavior in the voltage signals and proposed a detailed microscopic mechanism to elucidate it. Our strategy could benefit the development of nanopore technology and contribute to understanding the working principles of the units in a nanopore circuit system.

Introduction

Nanopore technology has emerged as a practical tool to detect and analyze single molecules such as nucleic acids,[1–4] proteins,[5–10] peptides,[11,12] and enzymes[13,14] due to its merits of high accuracy, low cost, and fast processing without extra PCR amplification and chemical labeling. Current nanopore detection is based on the method of resistive pulse sensing, which can be traced back to the Coulter counting used to count and measure particles in solution.[15] The core of this method is the current flow through the nanopores consisting of cations and anions moving under the electric field, which could be interfered with by analytes trapped inside the nanopore cavity, occupying the space of ions, and consequently, the absence of these ions causes a "current blockade" signal which will be reflected in the electrical circuit. Through examining the characteristics of this signal, for example, its amplitude of the current pulse, duration time, and the frequency of pulses, one can access much information about the analyte, such as size,[16] charge,[17] shape,[18] affinity with the nanopore wall,[8] dipole moments,[19] sequences of DNA and the concentration in the buffer solution.

The principle of the above-mentioned resistive pulse sensing method is the voltage clamp, an experimental way that clamps the value of voltage across the membrane and detects the varying transmembrane current. Conversely, another way is named the current clamp, which holds the value of current constant and measures the changes in the potential across the membrane.[20] The purpose of a current clamp is that it mimics the nature of the synaptic transmission, recording the resting potential in the presence of zero input current and the action potential elicited by a rectangular current pulse, thereby enabling monitoring of the ion channel activity. This method has been extensively used in research on biological ion channels.[21] In addition to that, the current clamp has been utilized in a wealth of applications. Gurunian *et al.* modeled the electroporation using the current clamp by analyzing the voltage fluctuations resulting from the creation of pores on the membrane across which a constant current is applied.[22] This fabrication strategy is referred to as controlled dielectric breakdown (CBD).[23] Arcadia *et al.* used the current clamp mode to conduct dielectric breakdown, which was self-limiting and reduced the pore formation time compared to the voltage clamp configuration.[24] Nevertheless, combining the solid-state nanopore technology and the current clamp approach to sensing biomolecules has not been reported yet, which could exhibit unexpected features compared with the voltage clamp.

The configuration of traditional nanopore sensing involves a set-up of single nanopore sandwiched between two reservoirs filled with buffer solutions, and in one of them biomolecules are added that will translocate the nanopore driven by electrophoretic/electroosmotic forces. Recently, integrating two or more nanopores into a circuit system has shown its superiority in biomolecule sensing. Langecker *et al.* first fabricated a nanodevice consisting of two stacked nanopores with a gap of

Jiangsu Key Laboratory for Design and Manufacture of Micro-Nano Biomedical Instruments, School of Mechanical Engineering, Southeast University, Nanjing 211189, China. E-mail: major212@seu.edu.cn

† Electronic supplementary information (ESI) available. See DOI: https://doi.org/10.1039/d2cp04530c

1.5 μm and then exploited them to generate two adjacent current blockade signals, which finally could determine the free-solution mobility of DNA on the basis of this "time-of-flight" (TOF) strategy.[25] Afterward, Choi *et al.* reported that the distance between two nanopores could influence the separation accuracy of molecules with different mobilities, showing an optimized length of 10 μm to discriminate four deoxynucleotide monophosphates.[26] These dual nanopore TOF sensors are actually a nanopore series circuit, while parallel nanopores are examined as well, termed "Tug-of-War". Zhang *et al.* first fabricated this "Tug-of-War" nanofluidic device and reported its two features: (i) sensing and resensing the same DNA molecule in sequence by two independent nanopores; (ii) cocapture of one DNA molecule by two nanopores and significantly extending the translocation time.[27] Choudhary *et al.* then increased the fidelity of loading and threading one DNA strand through double nanopores by designing two hourglass-shaped microchannels to retain the molecule and adding orthogonal pressure-driven flows above and below the nanopores, thereby delivering the molecule from the first nanopore to the second one successfully.[28] Apart from the dual-nanopore system, a quad-nanopore device was also designed, with four parallel nanopores slaved by programable voltage control, which enabled multiple detection modes such as sensing in a given channel sequence and trapping a DNA molecule along any two nanopores.[29] Hence, the double nanopore system serves as a potential tool for improving single molecule reading accuracy and offering multiple reading modes for the same analyte.

Here, we used the current clamp mode which records voltage blockade signals to sense biomolecules in solid-state nanopores for the first time. We also coupled this method with a serial nanopore circuit, which could monitor the blockade status of each nanopore. Furthermore, we discovered a new charging and discharging phenomenon in voltage blockade signals. To elucidate it, we proposed a novel mechanism of transmembrane potential polarization across the nanopore which well describes the physics during the DNA translocation. In terms of application, collision events and brief events caused by DNA fragments hinder the statistical analysis of DNA samples. Our voltage recording method could figure out this problem because these events hardly induce a high potential polarization, thereby increasing the fidelity of data. Our approach opens an avenue to record and analyze nanopore signals.

Results and discussion

Serial nanopore circuit

We built a serial nanopore circuit as illustrated in Fig. 1a. The two nanopores were clamped between three homemade flow cells, respectively. The applied total voltage (*i.e.*, the channel working under the voltage clamp mode) was set by immersing the positive electrode in one small cell and the ground electrode in the other small one. Hence, the total voltage was divided into two parts related to the resistance value of the two nanopores (*i.e.*, the nanopore with larger resistance gets more voltage). In this series circuit, the current is the same everywhere and could be recorded by the voltage clamp. The electrode of another channel working under the current clamp mode was inserted into the larger cell. Note that no input

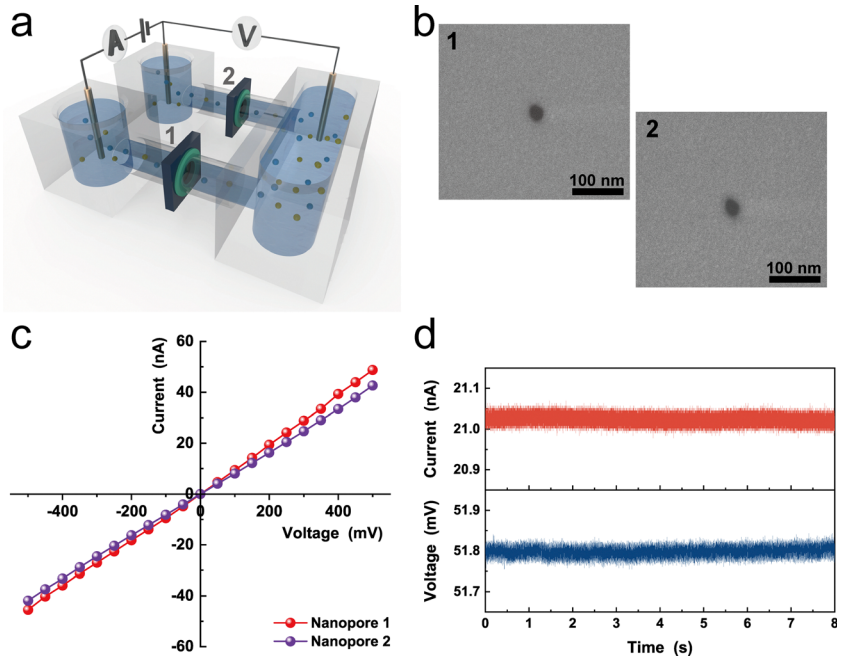

Fig. 1 Schematic diagram of the experimental setup to detect the DNA translocation signal. (a) Illustration of the serial nanopore circuit. (b) SEM figures of the two 20 nm-diameter nanopores drilled using FIB. (c) Measured *I*–*V* curves of the two nanopores in 1 M KCl solution from −500 mV to 500 mV with a step of 50 mV. (d) The current trace (red line) obtained under the voltage clamp mode and the corresponding voltage trace detected under the current clamp mode. The solution was 3 M LiCl.

current was set in this mode, so this channel served as a voltmeter basically. Therefore, the temporal voltage changes of one nanopore can be recorded.

In our experiment protocol, DNA fragments were added to the cell where the ground electrode was set. Driven by the electrophoretic force, DNA molecules would translocate the nanopore numbered 2 to the larger cell. When the DNA molecule was inside nanopore 2, the volume that had originally transported the ions was occupied, causing the ionic current to decrease instantaneously. In this serial circuit, the resistance of nanopore 2 increased temporarily since the nanopore size was narrowed by DNA, and the total resistance of the circuit would increase (although the resistance of nanopore numbered 1 remained unchanged). Considering that the applied voltage is constant, the entire current would decrease according to Ohm's law. This agrees with the principle of the resistive pulse sensing method. In terms of voltage, nanopore 2 would get more voltage due to its increment of resistance, based on the voltage division rule. This subtle change in the voltage was expected to be detected by the feedback amplifier. We also call this signal "voltage blockade". It is important to note that the voltage blockade signal is upward, the inverse direction of the current blockade.

Fig. 1b shows the SEM snapshots of the two nanopores, which were drilled using FIB using the same parameters (details of the structure of the nanopore membrane and the fabrication process are listed in the Methods section). To better control the voltage across a single pore, the diameters of the two pores were kept the same, which can be confirmed from SEM pictures and *I–V* curve measurements shown in Fig. 1c. The voltage sweep was taken from −500 mV to 500 mV step 50 mV in 1 M KCl solution, and the current–voltage curves show that the two pores have a similar size. Fig. 1d displays the bare current signal (upper red line) and voltage signal (lower blue line) without adding any DNA samples. The total applied voltage is 100 mV, and after voltage division, the voltage across nanopore 2 is 51.8 mV, demonstrating that it is a bit smaller than nanopore 1. We also examined the noise level of the voltage trace and compared it with that of the current trace, shown in ESI,† Fig. S1, which manifests that the voltage trace is competent in nanopore sensing similar to the current-based method.

Voltage blockade signal under the current clamp mode

Fig. 2a shows the current trace and the corresponding voltage trace after adding DNA samples (Nolimits 2500 bp) in the flow cell where the ground electrode was set. As mentioned before, the current trace was recorded by the voltage clamp applying varied voltage and the voltage trace was recorded by the current clamp applying no current. As expected, when DNA molecules translocate nanopore 2, a downward pulse signal occurs in the current trace while an upward pulse signal occurs simultaneously in the voltage trace. For true translocation events (*i.e.*, the DNA molecule translocates from one reservoir to another completely), each current blockade signal has a corresponding voltage blockade signal. For collision events (the DNA molecule diffuses to the pore mouth, knocks the exterior surface but moves back to the bulk), a short-time current blockade signal will occur but no voltage blockade signal emerges. We confirmed this conception through scatter plots of the blockade amplitude *versus* the dwell time, as shown in Fig. 2b. It is well known that DNA molecules present different conformations (unfolded or folded) when passing through the nanopore, and this will influence the value of the blockade amplitude and the dwell time. Nevertheless, the integral of the blockade amplitude with respect to the dwell time, also named event charge deficit (ECD), representing the total charge of the analyte, excludes the effect of conformation changes as it is only related to the length of DNA fragments which are uniformly charged in length.[30] We calculated the integral of all current blockade events and obtained an ECD value (equal to 0.019 pC) by Gaussian fitting of histograms of the integral distribution. As shown in Fig. 2b-(i), (iii) and (iv), scatters of the true translocation events distribute near the ECD curve (purple line) because those correspond to the DNA molecules fully translocating the nanopore and the entire charge can be recorded. However, shown in the areas marked by green circles, scatters of the collision events distribute far from the ECD curve as these molecules are captured only for a short time at the pore mouth and escape quickly, thereby inducing little blockade and short dwell time in signals. These collision events could lead to wrong judgments in the statistical analysis of translocation signals. Yet this problem would not occur in dealing with the voltage blockade signals. As shown in Fig. 2b-(ii), (iv) and (vi), no scatters of the collision events appear and all scatters distribute near a hyperbolic fitting curve. Note that the ECD curve could not be simply used in the scatter plot of voltage blockade signals because the dwell time of those is elongated which we will discuss later.

Compared with a single current blockade signal, this double check with another voltage blockade signal will potentially increase the fidelity of nanopore sensing. The dual-nanopore system was reported to examine translocation events by driving DNA molecules to translocate two adjacent nanopores in sequence and obtaining two near current blockade signals.[27] One problem of this method is that the reliability correlates with the nanopore gap since it may occur that another molecule in the middle volume translocates the second nanopore instead. Our strategy could avoid this problem as the distance between two nanopores is extremely long at the order of cm compared with that of μm in the dual-nanopore system. Moreover, if the DNA molecule diffuses to the vicinity of the second nanopore and passes through it, this would induce a downward voltage blockade signal because the current clamp monitors the voltage change of the first nanopore, the resistance of which is unchanged and then gets less voltage in voltage division. As shown in the voltage trace in Fig. 2a, no downward blockade signals are observed which reveals that actually, no molecules could diffuse to the second nanopore in the time range of 10 s. In addition, the selection of blockade events from the current/voltage trace complies with the same rule (the blockade amplitude divided by the noise level), thus it could not be that the collision events are filtered by different selection rules.

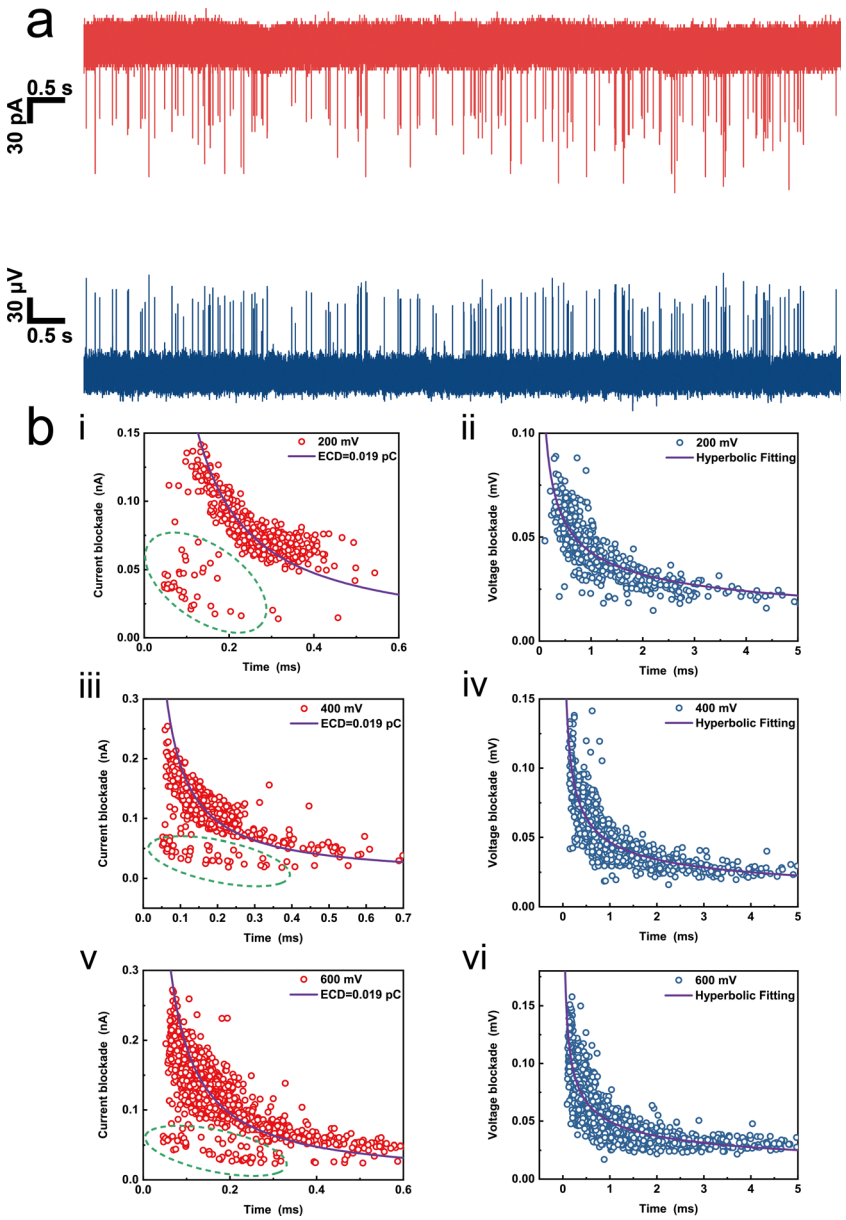

Fig. 2 Comparison of DNA translocation events between the current blockade signals under the voltage clamp mode and the voltage blockade signals under the current clamp mode. (a) A 10 s current trace (upper red line)/voltage trace (lower blue line) of DNA translocation events simultaneously recorded by the two channels of Axon MultiClamp 700B. (b) The scatter plots of the current blockade (i, iii and v) or the voltage blockade (ii, iv and vi) *versus* the dwell time inside the nanopore. The experiments were performed under different bias total voltages: (i and ii) 200 mV; (iii and iv) 400 mV; (v and vi) 600 mV. The purple lines in (i, iii and v) represent that the event charge deficit (ECD) of the translocation events is nearly constant and that lines in (ii), (iv) and (vi) are fitted by a hyperbola. The areas marked by green elliptical lines in (i), (iii) and (v) represent where collision events occur.

Charging and discharging phenomenon

We then focused on the specific blockade signals. We observed a novel charging and discharging phenomenon in the voltage blockade signals. As shown in Fig. 3a(i), when a DNA molecule translocates the nanopore, the current blockade signal appears as a downward pulse, while the corresponding voltage blockade signal shows an exponential rise and a subsequent exponential fall. This exponential curve of the voltage *versus* the time is similar to the mechanism of charging and discharging a capacitor. In general, a nanopore inserted in a membrane can be treated as a resistor in parallel with a capacitor, forming an RC parallel circuit. When a current flows through the nanopore, it first charges up the membrane capacitance, and then maintains the voltage across the membrane. Consequently, the voltage across the nanopore presents an exponential behavior. The voltage response $V(t)$ reads,

$$V(t)_{\text{Charing}} = V_{\text{eq}}(1 - \text{e}^{-t/\tau}) \quad (1)$$

$$V(t)_{\text{Discharing}} = V_{\text{eq}} \cdot \text{e}^{-t/\tau} \quad (2)$$

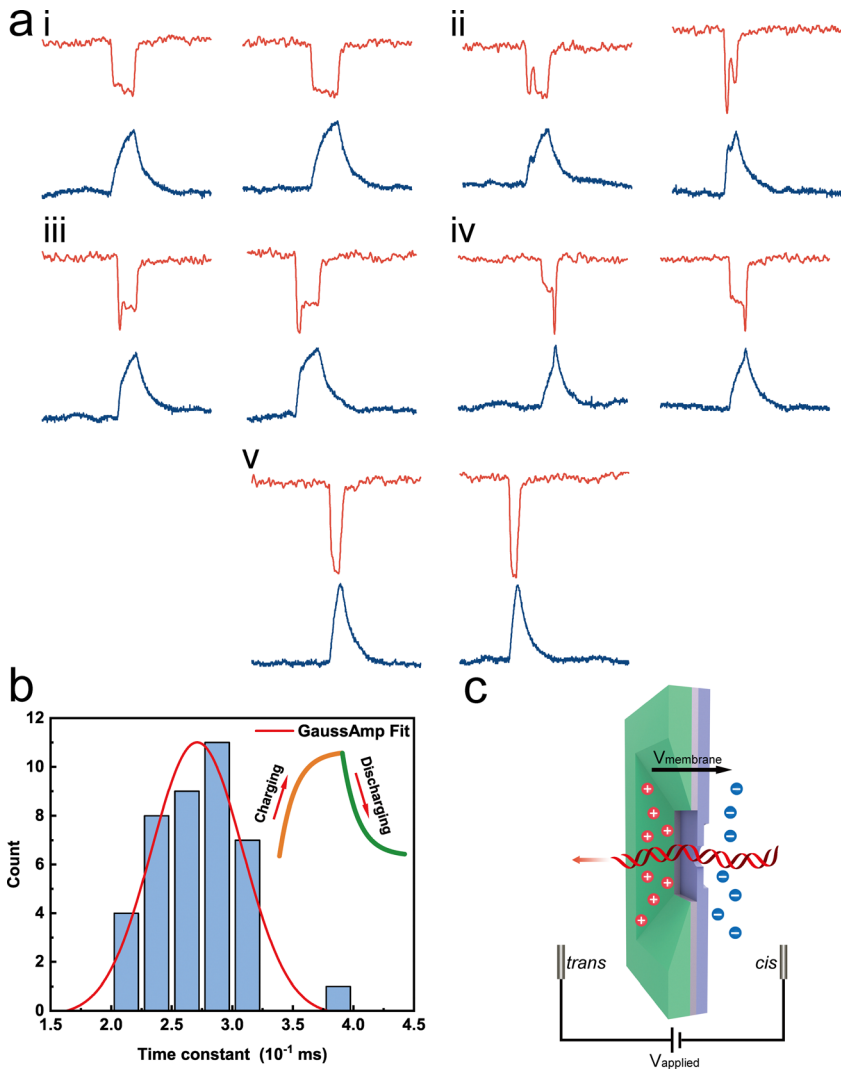

Fig. 3 Charging and discharging curves in the voltage blockade signals. (a) Five typical kinds of events representing different conformations inside the nanopore extracted from the raw traces of the DNA translocation. The upper red line is the current blockade signal while the lower blue line is the voltage blockade signal. (b) The frequency counts of the time constant were obtained from fitting 40 randomly selected events with the discharging equation. The red line is the Gaussian fitting of the histograms of the time constant. (c) Illustration of the microscopic mechanism of the charging and discharging phenomenon.

Here, V_{eq} is the voltage value when reaching the equilibrium and τ is the time constant representing the charging speed. In this RC parallel circuit, the voltage across the resistor is expected to increase immediately once the nanopore is blocked by the DNA molecule, but due to the presence of the capacitor, the voltage shows an exponential response, slowly rising to the equilibrium value. The time constant τ is the product of the nanopore resistance and the membrane capacitance, thus this charging and discharging process is intimately related to the characteristics of the nanopore.

To elucidate the charging and discharging phenomenon more thoroughly, we proposed a microscopic mechanism based on ion transport, as shown in Fig. 3c. When the DNA molecule enters the nanopore, it occupies the volume inside and blocks the path of the ion motion, and hence ions are continuously accumulating at the pore mouth (where the potential gradient is higher compared to the space near the membrane surface), with cations staying at the positive side and anions staying at the negative side. This accumulation of ions gives rise to the polarization effect, causing an additional transmembrane potential $V_{membrane}$ across the nanopore. As a consequence, the total voltage across the nanopore shows a continuous increase with the process of ion accumulation, which corresponds to the charging of the membrane capacitance. After the DNA molecule leaves, these abundant ions move through the nanopore, thus corresponding to the discharging process. For collision events, given that the DNA molecule blocks few ions outside the nanopore, it is hard to build a transmembrane potential, and hence induce an obvious voltage blockade signal.

In the charging period, the conformation of the DNA translocation will influence the charging curve, as shown in Fig. 3a. Fig. 3a(i) is the signal of a completely unfolded conformation,

where the charging curve is smooth. Similarly, in Fig. 3a(v), the curve of a fully folded conformation is continuous, but the slope of it is steeper, this is because the flux of ions passing through the nanopore is restricted more severely by the folded molecule, and hence the accumulation of ions at the pore mouth is faster. This could also be confirmed in the partly folded translocation events shown in Fig. 3-(iii) and (iv), where the charging curve consists of two parts with different slopes. When the DNA molecule enters the nanopore with a folded conformation and ends with an unfolded conformation (Fig. 3a(iii)), the curve starts with a fast charging period and then turns to a slow-down pattern. As expected, the curve in Fig. 3a(iv) shows the opposite trend.

In the discharging period, the conformation of the DNA translocation has no effect on the discharging curve as these five types of events all show the same pattern. This is because, at the start of the discharging process, the molecule has already left the nanopore which can be inferred by the comparison of the current signal and the voltage signal where the start point of discharging corresponds to the end of the current pulse. After the translocation, accumulated ions reoccupy the volume inside the nanopore to rebuild the equilibrium of the transmembrane potential, thus bringing the voltage to its original value. The relaxation time of this process equals the discharging time, and it can also be described by the time constant τ. We then fitted the discharging curves of forty events with eqn (2) and obtained a time constant of 0.28 ms, shown in Fig. 3b. This value is nearly four orders larger than the electromigration time for an ion to travel across the nanopore. This may be attributed to the moving of ions into the nanopore being successive and cannot be simply modeled as the motion of a single ion. Because of the extra discharging process, the dwell time of the voltage blockade signal is longer than that of the current blockade signal, which was mentioned in the scatter plots in Fig. 2b.

The method proposed in this work, *i.e.*, serial nanopore circuit combined with the current clamp, still has limitations. First, the bandwidth corresponding to the time constant 0.28 ms in this RC circuit is 568 Hz, which is relatively low. This may lead to the limitation that the signals of some fast-translocating molecules would be filtered. Nevertheless, modifying the parameters, nanopore resistance or membrane capacitance, may alleviate this limitation. Then, if applying this method to nanopores with small spacing (μm level), further efforts are needed to improve the fabrication technology of serial nanopores, especially inserting conducting wires between them. Furthermore, several specific scenarios should be considered. For example, two or more DNA molecules translocate different pores at the same time, or one of these multi pores is clogged. It is also worthwhile to investigate how the membrane capacitance or the nanopore self-capacitance influences the voltage blockade signals of the DNA translocation since this could figure out how the system maintains charge neutralization when an external charge carrier (DNA molecules) invades.

In summary, we proposed a new strategy combining a nanopore series circuit and a current clamp to obtain the current trace and the voltage trace through a nanopore simultaneously. Compared with current signals, the voltage signals can successfully exclude the collision events of DNA translocation and thus increase the fidelity of event analysis. The specific profile of the voltage signal presented a charging and discharging characteristic, for which we gave a microscopic mechanism based on the polarization potential to explain. Our work may inspire the strategies and technologies in single-molecule detection.

Methods

Nanopore fabrication

The nanopore membrane is fabricated through a MEMS process. A 1 μm-thick SiO_2 membrane was deposited on a bare Si wafer by thermal oxidation. Then, a 100 nm-thick Si_3N_4 membrane was grown on the SiO_2 layer through LPCVD (low-pressure chemical vapor deposition). The front Si_3N_4 membrane was selectively etched, with the thickness of a 2 μm-diameter area reduced to 20 nm by reactive ion etching which corresponds to the thickness of the nanopore. The back side of the wafer was etched to remove the deposition layers and expose the bottom of the front Si_3N_4 membrane by photolithography and wet etching. Finally, a 40 μm × 40 μm free-standing Si_3N_4 membrane was obtained. The SiO_2 layer was designed to reduce the parasitic capacitance and increase the signal-to-noise ratio of nanopore sensing current. A nanopore with a diameter of 20 nm was drilled on the center of the Si_3N_4 membrane using FIB (Focus Ion Beam, FEI Helios Nanolab 600i) with a time parameter of 30 ms and the beam current set at 1.1 pA. Before experiments, the nanopore chips were treated with piranha solution (H_2O_2/H_2SO_4, 1 : 3) at 120 °C for 1 h to remove surface contaminants and subsequently washed with ethanol and deionized water both three times. Then, the nanopore chips were treated with 100 W oxygen plasma for 20 s. These two steps facilitated the formation of polar bonds (Si–OH) on the Si_3N_4 membrane surface, which enhanced the surface hydrophilicity and minimized the effect of bubble formation.

Electric circuit

A home-made polymethylmethacrylate (PMMA) device including two small flow cells and one larger counterpart was fabricated to connect the two nanopores, forming a serial nanopore circuit, as shown in Fig. 1a. Each nanopore chip was clamped between a small flow cell and the larger one, with silicone elastomer gaskets sealing the contact area. The electrolyte solution was filled into all flow cells, and three Ag/AgCl electrodes were immersed into the cells respectively to build the electric circuit. The positive electrode of the voltage clamp was set in one small cell and the ground electrode was set in the other one to apply a total voltage between two nanopores. Hence, the two nanopores were resistors connected in series which divided the total voltage into two parts according to the nanopore resistance. The positive electrode of the current clamp was set in the larger flow cell and the current input was set to zero, which meant it served as a voltammeter detecting the temporal voltage change of one nanopore. Ionic current signals were recorded by one channel working in the voltage clamp mode of the resistive feedback

amplifier (Axon MultiClamp 700B), and voltage signals were recorded by another channel working in the current clamp mode. The data were sampled at 250 kHz by Digidata 1550A, Molecular Devices, and lowpass filtered at 10 kHz. All the experiments were performed in a dark Faraday cage.

Reagents

The salt solution used in experiments was prepared using deionized water (18.2 MΩ cm, Milli-Q IQ 7000 ultrapure water system) and degassed, filtered, and adjusted to pH 8 at room temperature. The DNA fragments (Fermentas Nolimits^{TM} 2500 bp & Lambda DNA) were purchased from Sangon Biotech Co., Ltd. The DNA fragments were added to a buffer solution (3 M LiCl, 10 mM Tris-HCl & 1 mM EDTA). Before experiments, the samples were heated in a 60 °C water bath for 3 min and then cooled in an ice water bath for 10 min to allow DNA molecules to disperse in the solution completely. Between experiments using different samples, the chambers of the flow cell were washed with the buffer solution three times and the open pore current was monitored for 10 min to ensure no residual molecules were present in the chamber.

Author contributions

J. S. and F. Z. proposed the idea to use a nanopore series circuit to detect DNA translocation. F. Z. and W. X. performed the device fabrication and DNA translocation experiments. F. Z., Y. T., and J. S. conducted the data analysis. F. Z. and J. S. co-wrote the manuscript. All authors discussed the results and commented on the manuscript.

Conflicts of interest

The authors declare no competing financial interests.

Acknowledgements

The authors thank the Natural Science Foundation of China (52075099, 52035003, and 51705074) for financial support. Fei Zheng is supported by the Postgraduate Research & Practice Innovation Program of Jiangsu Province (Grant No. KYCX20_0081).

References

1 J. J. Kasianowicz, E. Brandin, D. Branton and D. W. Deamer, *Proc. Natl. Acad. Sci. U. S. A.*, 1996, **93**, 13770.
2 J. Clarke, H.-C. Wu, L. Jayasinghe, A. Patel, S. Reid and H. Bayley, *Nat. Nanotechnol.*, 2009, **4**, 265.
3 C. Cao, Y.-L. Ying, Z.-L. Hu, D.-F. Liao, H. Tian and Y.-T. Long, *Nat. Nanotechnol.*, 2016, **11**, 713.
4 M. Wanunu, T. Dadosh, V. Ray, J. Jin, L. McReynolds and M. Drndić, *Nat. Nanotechnol.*, 2010, **5**, 807.
5 B. Hornblower, A. Coombs, R. D. Whitaker, A. Kolomeisky, S. J. Picone, A. Meller and M. Akeson, *Nat. Methods*, 2007, **4**, 315.
6 C. B. Rosen, D. Rodriguez-Larrea and H. Bayley, *Nat. Biotechnol.*, 2014, **32**, 179.
7 M. Rahman, M. A. Stott, M. Harrington, Y. Li, M. J. N. Sampad, L. Lancaster, T. D. Yuzvinsky, H. F. Noller, A. R. Hawkins and H. Schmidt, *Nat. Commun.*, 2019, **10**, 1.
8 R. Wei, V. Gatterdam, R. Wieneke, R. Tampé and U. Rant, *Nat. Nanotechnol.*, 2012, **7**, 257.
9 N. Varongchayakul, J. Song, A. Meller and M. W. Grinstaff, *Chem. Soc. Rev.*, 2018, **47**, 8512.
10 J. Lei, Y. Huang, W. Zhong, D. Xiao and C. Zhou, *Anal. Chem.*, 2020, **92**, 8867.
11 M. Kukwikila and S. Howorka, *Anal. Chem.*, 2015, **87**, 9149.
12 A. Fennouri, J. List, J. Ducrey, J. Dupasquier, V. Sukyte, S. F. Mayer, R. D. Vargas, L. Pascual Fernandez, F. Bertani and S. Rodriguez Gonzalo, *ACS Nano*, 2021, **15**, 11263.
13 T. C. Sutherland, Y.-T. Long, R.-I. Stefureac, I. Bediako-Amoa, H.-B. Kraatz and J. S. Lee, *Nano Lett.*, 2004, **4**, 1273.
14 A. Fennouri, C. Przybylski, M. Pastoriza-Gallego, L. Bacri, L. Auvray and R. Daniel, *ACS Nano*, 2012, **6**, 9672.
15 L. Xue, H. Yamazaki, R. Ren, M. Wanunu, A. P. Ivanov and J. B. Edel, *Nat. Rev. Mater.*, 2020, **5**, 931.
16 X. Lin, A. P. Ivanov and J. B. Edel, *Chem. Sci.*, 2017, **8**, 3905.
17 Y. Wang, Y. Wang, X. Du, S. Yan, P. Zhang, H.-Y. Chen and S. Huang, *Sci. Adv.*, 2019, **5**, eaar3309.
18 J. Sha, W. Si, B. Xu, S. Zhang, K. Li, K. Lin, H. Shi and Y. Chen, *Anal. Chem.*, 2018, **90**, 13826.
19 J. Houghtaling, C. Ying, O. M. Eggenberger, A. Fennouri, S. Nandivada, M. Acharjee, J. Li, A. R. Hall and M. Mayer, *ACS Nano*, 2019, **13**, 5231.
20 M. Devices, *Sunnyvale MDS Anal. Technol*, 2008.
21 F. Frohlich, *Network Neuroscience*, Academic Press, 2016.
22 A. Gurunian and D. A. Dean, *Bioelectrochemistry*, 2022, 108162.
23 H. Kwok, K. Briggs and V. Tabard-Cossa, *PLoS One*, 2014, **9**, e92880.
24 C. E. Arcadia, C. C. Reyes and J. K. Rosenstein, *ACS Nano*, 2017, **11**, 4907.
25 M. Langecker, D. Pedone, F. C. Simmel and U. Rant, *Nano Lett.*, 2011, **11**, 5002.
26 J. Choi, Z. Jia, R. Riahipour, C. J. McKinney, C. A. Amarasekara, K. M. Weerakoon-Ratnayake, S. A. Soper and S. Park, *Small*, 2021, **17**, 2102567.
27 Y. Zhang, X. Liu, Y. Zhao, J.-K. Yu, W. Reisner and W. B. Dunbar, *Small*, 2018, **14**, 1801890.
28 A. Choudhary, H. Joshi, H.-Y. Chou, K. Sarthak, J. Wilson, C. Maffeo and A. Aksimentiev, *ACS Nano*, 2020, **14**, 15566.
29 P. Cadinu, M. Kang, B. P. Nadappuram, A. P. Ivanov and J. B. Edel, *Nano Lett.*, 2020, **20**, 2012.
30 N. A. Bell, M. Muthukumar and U. F. Keyser, *Phys. Rev. E*, 2016, **93**, 022401.

